

Experimental Investigation on Combustion and NO_x Formation Characteristics of Low-Ash-Melting-Point Coal in Cyclone Furnace

Limin Wang, Chunli Tang,* Tao Zhu, Fan Fang, Xing Ning, and Defu Che

Cite This: *ACS Omega* 2022, 7, 26537–26548

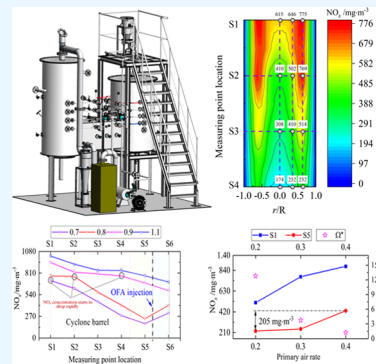
Read Online

ACCESS |

Metrics & More

Article Recommendations

ABSTRACT: Slag tapping cyclone furnace is suitable and promising for the utilization of low-ash-melting-point coals without worrying about the fouling and slagging problems, but its high NO_x emission has limited its application. In this study, the temperature profiles, species concentration distributions, and slag tapping behavior of the cyclone barrel were explored on a self-built 100 kW cyclone furnace system. A reasonable slag capture ratio of 0.70 can be achieved for the cyclone barrel even under air-staged conditions. The coincidence of high temperature and high O₂ concentration in the annular near-wall area of the cyclone barrel can lead to a large amount of NO_x formation, while a NO_x reduction area with high CO concentration is formed in the central and lower zones of the cyclone barrel due to strong swirling effect. The NO_x emission of cyclone staged combustion is lower than that of laminar drop-tube staged combustion in either air-staged or nonstaged cases, which could be attributed to the swirling effect. The NO_x reduction area can be expanded by decreasing the cyclone stoichiometric ratio (SR) or reducing the primary air rate (PAR). Compared with the limit effects on the reduction of NO_x emission by overall-SR, NO_x formation can be greatly dropped by 56% when the cyclone-SR decreases from 1.1 to 0.7. The swirling intensity in cyclone barrel increases from 1.23 to 12.81 as PAR reduces from 0.4 to 0.2, which results in a reduction of NO_x formation at the outlet of the cyclone barrel by half. Besides, the O₂ concentration in the annular near-wall region can be remarkably reduced by the decentralized secondary air supply, resulting in a 23% reduction in NO_x formation in the cyclone barrel.



1. INTRODUCTION

Low-ash-melting-point coal accounts for one-third of coal reserves in China,^{1,2} which will continue to play an important role as a “ballast stone” to ensure future energy security of China. For example, as a kind of low-ash-melting-point coal, the typical Zhundong coal with a melting point between 1100 and 1200 °C has attracted the attention of many scholars.^{1,2} Unfortunately, the combustion of low-ash-melting-point coal is likely to cause serious fouling and slagging problems in pulverized coal boilers and circulating fluidized bed boilers. In contrast, the slag tapping cyclone furnace is quite suitable for the combustion of low-ash-melting-point coal.³ In the cyclone furnace, the molten ash formed by the combustion of low-ash-melting-point coal will deposit on the wall of the cyclone barrel under the action of a strong swirling effect and eventually be discharged in the form of liquid slag. The formed slag layer can insulate and protect the refractory material, which promotes the stable and safe operation of the cyclone furnace.^{4–6} Hence, the cyclone furnaces are ideal for burning low-ash-melting-point coals without worrying about fouling and slagging problems. However, the high combustion intensity of cyclone combustion can lead to a higher temperature, which may further result in higher NO_x emissions in cyclone furnaces. Therefore, it is of great significance to propose solutions to

reduce the NO_x formation in the cyclone furnaces for the safe and clean utilization of the low-ash-melting-point coal.

In recent years, a large number of studies have indicated that high-temperature combustion does not necessarily trigger the formation of a large amount of NO_x, but ultralow NO_x formation can be achieved for high-temperature combustion in a strong reducing atmosphere.^{7,8} The high temperature can promote the generation of substantial CO and C_xH_y by the gasification of the char in reducing atmosphere. C_xH_y would further enhance the homogeneous reduction of NO_x^{9–11} while CO could strengthen the heterogeneous reduction of NO_x by char.^{12–15} The experiment conducted by Taniguchi et al.^{11,16} on the drop tube furnace showed that the NO_x formation can be reduced effectively with the increase in the temperature of the fuel-rich zone under staged conditions. Bai et al.¹⁷ indicated that when the temperature was 1600 °C and the stoichiometric ratio (SR) in the fuel-rich zone was 0.7, the

Received: April 30, 2022

Accepted: July 6, 2022

Published: July 19, 2022



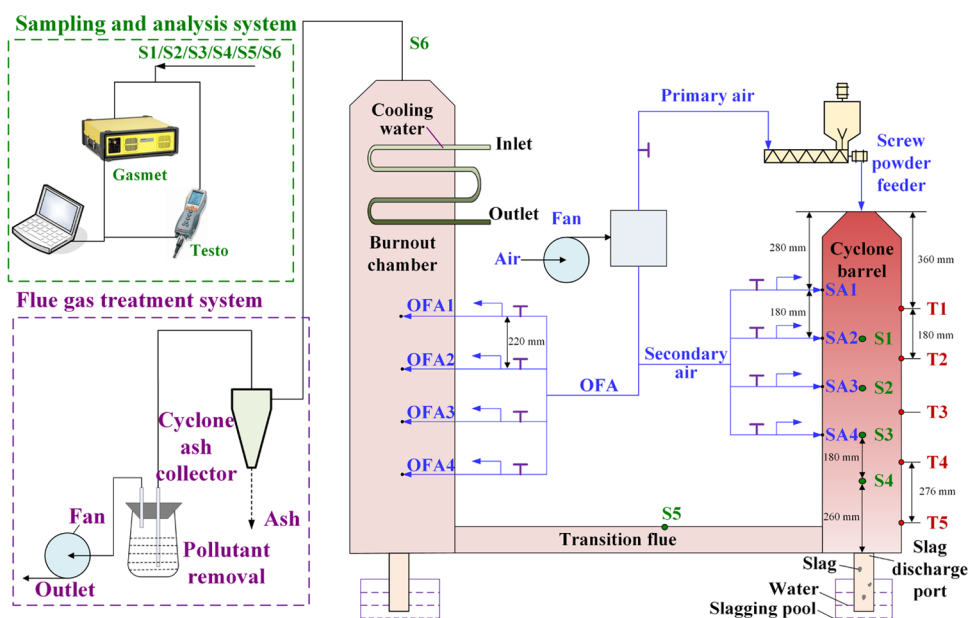


Figure 1. Experiment system diagram.

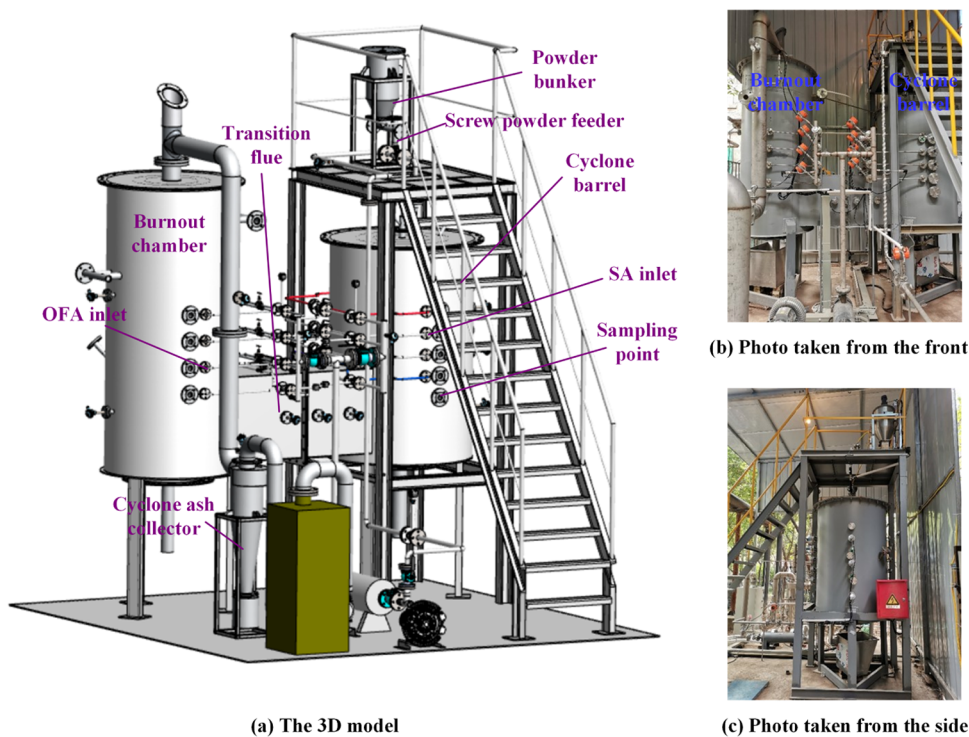


Figure 2. 3D model and photos of the cyclone furnace system.

NO_x formations for combustion of bituminous coal and anthracite were lower than $150 \text{ mg}\cdot\text{m}^{-3}$ and $360 \text{ mg}\cdot\text{m}^{-3}$, respectively. Zhu et al.¹⁵ separately investigated the fuel NO_x and thermal NO_x formations and indicated that high-temperature combustion will not cause high thermal NO_x at a low SR due to the insufficient oxygen concentration. They attributed the ultralow NO_x formation to the fact that the release of N is mainly in the form of volatile N at high temperatures, which can be easily reduced by Char, C_xH_y , and CO in a reducing atmosphere. Hence, the ultralow NO_x formation can be obtained under high temperatures and strong reducing atmosphere. In fact, unlike the pulverized coal

boilers and the circulating fluidized bed boilers for which it is difficult to simultaneously achieve both the strong reducing atmosphere and high-temperature conditions, the cyclone furnace can easily achieve both at the same time, which might be beneficial for achieving ultralow NO_x formation.^{18–20} However, most of the research related to NO_x formation was carried out in drop tube electric heating furnaces, which cannot directly guide the situation of strongly swirling combustion in cyclone barrels.

Some work has been devoted to the flow field characteristics in cyclone barrels. Krasinsky et al.^{21,22} experimentally studied the aerodynamic field in a designed cyclone combustion

furnace and characterized the swirling properties of the airflow, but they did not focus on the NO_x formation. Some other investigators have explored the NO_x formation in cyclone barrels. National Energy Technology Laboratory of the United States Department of Energy (DOE/NETL) reported that the NO_x formation of a 138 MW cyclone furnace can be reduced by 52% when air-staged combustion was used.²³ The research conducted by Babcock & Wilcox B&W company^{24–26} also showed that the NO_x formation can be reduced efficiently to 108 ppm when the SR was reduced to 0.7. Zhu et al.²⁷ also showed that staged combustion can effectively decrease the NO_x formation in the cyclone barrel. However, the above work only obtained the final NO_x formation values without analyzing the combustion characteristics and their effects on the NO_x formation in the cyclone barrel. According to our previous numerical simulation studies,^{6,28,29} the flow and combustion characteristics in the cyclone furnace are quite special due to the strong swirling aerodynamic field, which might greatly influence the formation of NO_x . Therefore, an in-depth experimental study of the combustion characteristics and their effects on the NO_x formation in the cyclone barrel is urgently needed for revealing the mechanism of NO_x formation in the cyclone combustion and further proposing strategies for reducing NO_x .

In this study, a 100 kW cyclone combustion furnace experimental system was built. The temperature profiles, species concentration distributions, and slag tapping behavior of the cyclone barrel were examined in detail. The effects of the overall stoichiometric ratio (overall-SR) and cyclone stoichiometric ratio (cyclone-SR) on NO_x formation were analyzed. The mechanisms of NO_x formation and reduction in the cyclone combustion process were discussed. Potential strategies for NO_x reduction were proposed and verified. This research will be beneficial to the safe and clean utilization of the low-ash-melting-point coal in cyclone furnaces.

EXPERIMENT AND METHOD

2.1. Experiment System. The cyclone combustion furnace experiment system is mainly composed of a furnace, fuel and air feeding system, flue gas treatment system, and sampling and analysis system, as shown in Figure 1. The 3D model diagram and pictures are shown in Figure 2. The details of the experiment system are as follows.

2.1.1. Furnace. The furnace is composed of a cyclone barrel, a transition flue, and a burnout chamber. For the cyclone combustion, the ash particles carried by strong swirl of air spun forward in the cyclone barrel. There is a slagging pool at bottom of the cyclone barrel, which is used to collect the slag discharged from the slag discharge port. The cyclone ash collector is arranged at the exit of the burnout chamber for collecting ash, as shown in Figure 1.

The cyclone furnace in this experiment was designed by scaling down the actual cyclone furnace to 1/7 according to the reference manual.²⁹ The detailed structure parameters can be found in Table 1. Refractory material was ranged on the fireside of the furnace. The furnace wall was composed of refractory material, insulation material, and steel plates. Corundum with the characteristics of high-temperature resistance and wear resistance was selected as the refractory material of the cyclone barrel to protect the furnace wall from deposition and erosion of the high-temperature molten slag. The cyclone barrel was coated with thermal insulation material of mullite carbon fiber. Silicon carbide with moderate

Table 1. Structural Parameters of the Cyclone Furnace

item	parameter	value
cyclone barrel	inner diameter/Height (mm)	280/1260
	material of refractory	corundum
	thickness of refractory material (mm)	100
	material of heat insulator	mullite fiber cotton
transition flue	thickness of heat insulator (mm)	350
	inner diameter/Length (mm)	120/1820
	material of refractory	silicon carbide
	thickness of refractory material (mm)	100
burnout chamber	material of heat insulator	aluminum carbonate fiber cotton
	thickness of heat insulator (mm)	200
	inner diameter/height (mm)	450/1800
	material of refractory	silicon carbide
burnout chamber	thickness of refractory material (mm)	100
	material of heat insulator	aluminum carbonate fiber cotton
	thickness of heat insulator (mm)	200

temperature resistance and wear resistance was selected as the refractory material for the transition flue and the combustion chamber, considering that only a small amount of ash particles would flow into the transition flue and the burnout chamber resulting in slight wear on the inner wall. Moreover, the temperatures of flue gas in the transition flue and the burnout chamber were much lower than that in the cyclone barrel. Aluminum carbonate fiber cotton was coated outside the transition flue and burnout chamber for thermal insulation.

2.1.2. Fuel and Air Feeding System. The ground and dried coal particles were fed into the cyclone barrel through the screw powder feeder, which was controlled by a motor, as shown in Figures 1 and 2. To ensure the stability and accuracy of the fuel feeding, the calibration of fuel feeding rate was performed, as shown in Figure 2. The fuel feeding rate of powder feeder is linearly correlated with motor frequency with tiny repeat error ($\pm 3\%$) in the range of fuel mass flow rate of 5–20 $\text{kg}\cdot\text{h}^{-1}$, indicating that the powder feeder can meet the experimental requirements (Figure 3).

The air was provided by the high-pressure fan. The arrangement of the air inlets is shown in Figure 1. The primary air was sent into the cyclone barrel from the inlet of primary air, which was arranged on the top of the cyclone barrel. The secondary air was sent into the cyclone barrel tangentially, causing the strong swirl airflow. Four layers of tangentially arranged secondary air (SA) inlets were arranged along the height of the cyclone barrel, and there were two secondary air inlets on each layer. The over fired air (OFA) was sent into the burnout chamber for burnout. Four layers of OFA air inlets were arranged along the height of the burnout chamber, and there are two OFA air inlets oppositely arranged to each other on each layer. The mass flow rate data were measured by vortex flowmeters, and the air flow mass rate was varied by adjusting the valves according to the experimental conditions.

2.1.3. Fuel Gas Treatment System. To protect the exhaust fan from the damage of high-temperature flue gas, water-

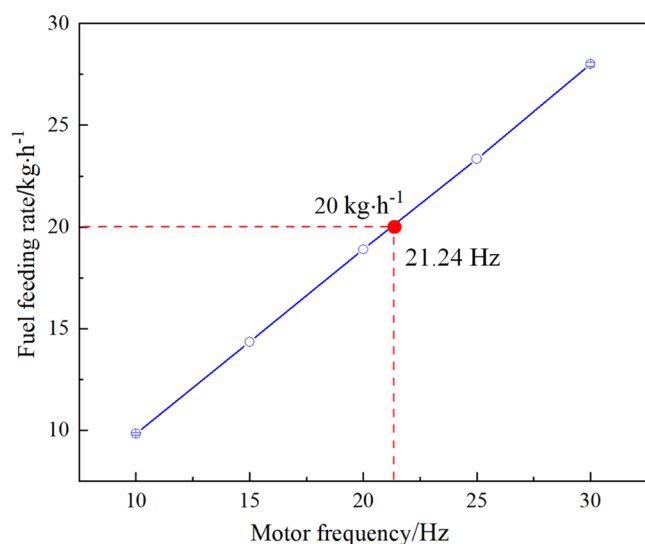


Figure 3. Calibration of fuel feeder.

cooled tubes were arranged on the top of the burnout chamber for cooling the high-temperature flue gas. The ash in the flue gas was collected efficiently by the cyclone ash collector. Then, the flue gas was discharged by the exhaust fan after pollutant removal.

2.1.4. Sampling and Analysis System. To obtain the temperature distribution in the cyclone barrel, four temperature measuring points with B-type thermocouples marked by T1, T2, T3, T4, and T5 were arranged along the side of the cyclone barrel, as shown in Figure 1. Besides, four sampling ports were evenly arranged along the height of the cyclone barrel and two sampling ports were arranged in the transition flue and the top of the burnout chamber, respectively. The flue gas can be extracted from the sampling ports and the flue gas constituent (NO, O₂ and CO) can be analyzed online by the flue gas analysis device (Gasetm and Testo).

2.2. Experimental Procedure and Conditions. As shown in Figure 4, before the experiment, the propane was burned to preheat the furnace. The flue gas temperature rose suddenly from the initial temperature (440 °C) to 723 °C once propane was burned. Subsequently, the temperature continued to rise for about 240 min. Temperature growth slowed down when the temperature reached 1170 °C. At this time, the

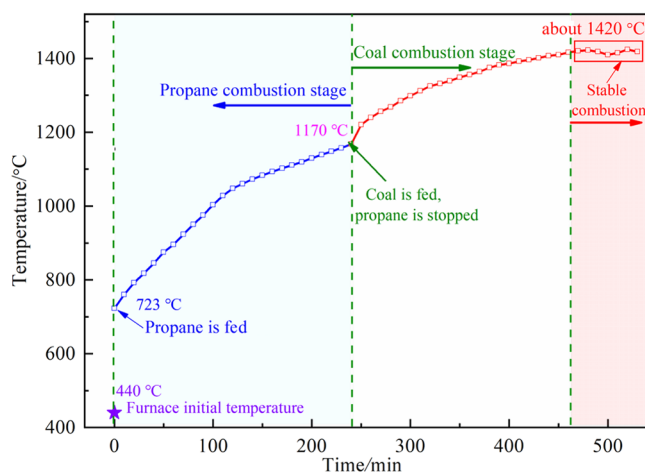


Figure 4. Temperature rising curve.

supply of propane was stopped and the pulverized coal was supplied. After pulverized coal burned, the flue gas temperature rose rapidly. The flue gas temperature continued to rise for 220 min and finally stabilized at 1420 °C.

In this study, the design value of the cross-sectional heat load of the cyclone barrel was 1.71 MW·m⁻². The thermal power of the cyclone furnace was 100 kW, which was achieved by the coal feeding rate of 20 kg·h⁻¹ and the total air mass flow rate of 123 m³·h⁻¹, with an overall-SR of 1.1. The working condition of the cyclone barrel with the SR of 0.8 was selected as the reference condition. The negative pressure in the furnace was controlled in the range of -50 to -100 Pa by adjusting the opening of the blower and induced draft fan. The main parameters of the experimental conditions are shown in Table 2. Hongshaquan coal was selected as research coal, and

Table 2. Main Parameters of the Experiment

item	unit	value
coal		Hongshaquan coal
mass flow rate of coal	kg·h ⁻¹	20
overall-SR		1.05, 1.1 (reference condition), 1.2
cyclone-SR		0.7, 0.8 (reference condition), 0.9, 1.1
primary air ratio		0.2, 0.3 (reference condition), 0.4
Reference Condition		
total air flow rate	kg·h ⁻¹	123
mass flow rate of primary air	kg·h ⁻¹	36.9
mass flow rate of SA1	kg·h ⁻¹	26.3
mass flow rate of SA2 (or SA3)	kg·h ⁻¹	26.3
mass flow rate of SA4	kg·h ⁻¹	0
mass flow rate of OFA1	kg·h ⁻¹	16.8
mass flow rate of OFA2	kg·h ⁻¹	16.8
mass flow rate of OFA3/OFA4	kg·h ⁻¹	0

its properties are shown in Table 3. Since Hongshaquan coal is a kind of low-ash-melting-point coal with an ash fusion

Table 3. Properties of Hongshaquan Coal

proximate analysis (dry basis) (wt %)		ash composition (wt %)	
fixed carbon	55.21	SiO ₂	39.77
volatile matter	35.99	Al ₂ O ₃	16.73
ash	8.80	Fe ₂ O ₃	13.93
		CaO	8.89
		MgO	5.55
ultimate analysis (dry basis) (wt %)			
carbon	72.09	Na ₂ O	5.34
hydrogen	4.20	K ₂ O	0.61
oxygen	13.44	TiO ₂	0.95
nitrogen	0.98	SO ₃	7.47
sulfur	0.49		
lower heating value (dry ash-free basis) (MJ·kg ⁻¹)	27.40	ash fusion temperatures (°C)	
		deformation temperature, DT	1096
		softening temperature, ST	1107
particle size distribution		flow temperature, FT	1114
mean diameters (μm)	49.13		
D ₉₀ (μm)	110.4		

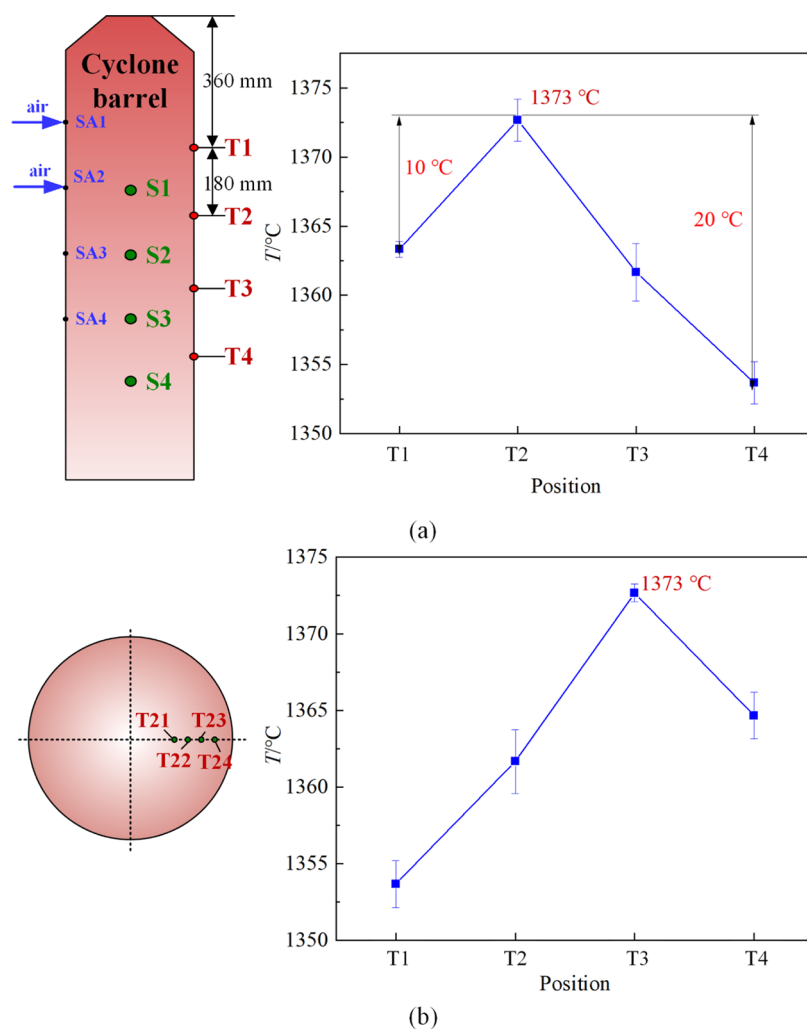


Figure 5. Temperature distribution in the cyclone barrel: (a) in the axial direction and (b) in the radial direction.

temperature lower than 1200 °C, it is easy to achieve liquid slagging during combustion in the cyclone barrel.

2.3. Analysis Method. For the convenience of analysis, the measured NO concentration value ($\mu\text{L}\cdot\text{L}^{-1}$) is converted into the corresponding NO_2 concentration value ($\text{mg}\cdot\text{m}^{-3}$), which is computed by

$$\text{NO}_2(\text{mg}\cdot\text{m}^{-3}) = C_{\text{NO}} \times \frac{M_{\text{NO}_2}}{M} \quad (1)$$

where C_{NO} is the measured concentration of NO, $\mu\text{L}\cdot\text{L}^{-1}$; M_{NO_2} is the molar mass of NO_2 , $\text{g}\cdot\text{mol}^{-1}$; and M is the molar volume of gas, $\text{L}\cdot\text{mol}^{-1}$.

The dimensionless swirling intensity in the cyclone barrel is expressed as

$$\Omega^* = \frac{8\bar{w}R_{\text{sw}}}{\pi D\bar{u}} \quad (2)$$

where \bar{w} and \bar{u} are, respectively, the mean tangential velocity and axial velocity, $\text{m}\cdot\text{s}^{-1}$; R_{sw} is the radius of swirling flow, m; and D is the diameter of the cyclone barrel, m.

3. RESULTS AND DISCUSSION

3.1. Temperature Profile in the Cyclone Barrel. The cyclone barrel is the main combustion site of the cyclone furnace, and the temperature distribution in the cyclone barrel

has significant effects on the NO_x formation and slag behavior. Figure 5 shows the temperature distribution in the cyclone barrel in the reference condition (namely, overall-SR of 1.1, cyclone-SR of 0.8, and PAR of 0.3). Along the height of the cyclone barrel, the temperature gradually increases from 1363 °C at T1 to a peak of 1373 °C at T2 and then gradually decreases to 1353 °C at T4, as shown in Figure 5a. The introduction of secondary air will induce the intense combustion of coal particles, resulting in the highest flue gas temperature at T2. Subsequently, as O_2 is gradually consumed, the lower part of the cyclone will be in an oxygen-lean atmosphere under the condition of cyclone-SR less than 1. Since the gasification reaction of pulverized coal is an endothermic reaction, the flue gas temperature decreases slightly. Furthermore, to investigate the radial temperature distribution in the cyclone barrel, the temperatures are measured at the points of 90, 70, 50, and 30 mm (marked as T21, T22, T23, and T24) radially from the wall at the height of sampling point T2. The temperature distribution in the radial direction is shown in Figure 5b. The flue gas temperature rises from 1365 °C at T24 to 1373 °C at T23 and then decreased to 1354 °C. The maximum radial temperature occurs at 50 mm away from the cyclone barrel wall. Most of the coal particles are driven to the area close to the barrel wall by the strong swirl and burned with relatively

sufficient O_2 . As a result, the central region with relatively lower temperature and the near-wall region with relatively higher temperature are formed in the cyclone barrel, which is same as our previous numerical simulation work.²⁸ The high temperature near the barrel wall is conducive to the formation of the slag layer, which is a key to the safe operation of the cyclone furnace.

Figure 6 shows the temperature of flue gas at the center and near the slagging port of the cyclone barrel under different

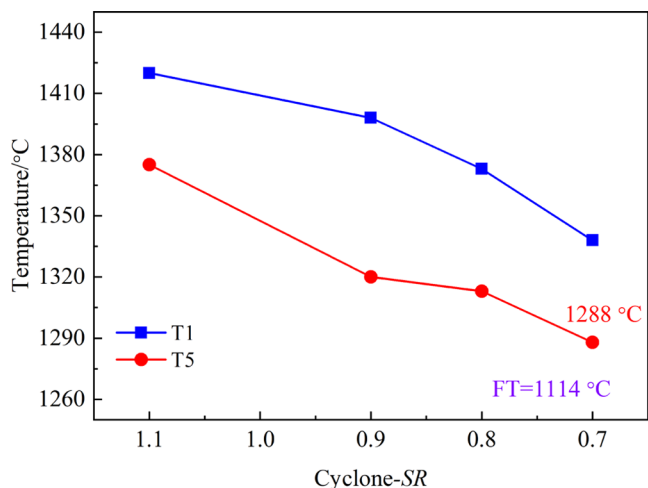


Figure 6. Effects of cyclone-SR on the temperature in the cycle barrel.

cyclone-SR conditions. Reducing the cyclone-SR from 1.1 to 0.7 can greatly decrease the temperature by 82 and 87 °C at the center and near the slagging port, respectively, as coal combustion is restrained under the oxygen lack conditions. Even in the case cyclone-SR of 0.7, the flue gas temperature at the center and bottom of cyclone can reach 1338 and 1288 °C, which are higher than the slag flow temperature of the research coal and ensure the slag tapping smoothly. In addition, the CO concentrations in the flue gas at the outlet of the cyclone furnace were 130 and 2790 $\mu\text{L}\cdot\text{L}^{-1}$, respectively. Therefore, considering the burnout characteristics and NO_x generation comprehensively, in the case of cyclone-SR of 0.8, low NO_x formation can be achieved at the premise of the acceptable incomplete combustion loss.

3.2. Slag Discharge Behavior. Under the action of a strong swirling effect in the cyclone barrel, most of the molten ash particles with a large particle size will deposit on the wall and further form the slag layer. The liquid slag will be discharged from the slag discharge port at the bottom of the cyclone barrel before and after the experiment are shown in Figure 7a,b, respectively. The inner wall pictures of the cyclone barrel before and after the experiment, whereas there was slag deposited on the wall of the cyclone barrel after the experiment. As the morphology of the slag in the photos shows, the slag flows downward under the action of gravity in the cyclone barrel.

The slag has been collected from the slagging pool and barrel inside wall, as shown in Figure 7c, from which the

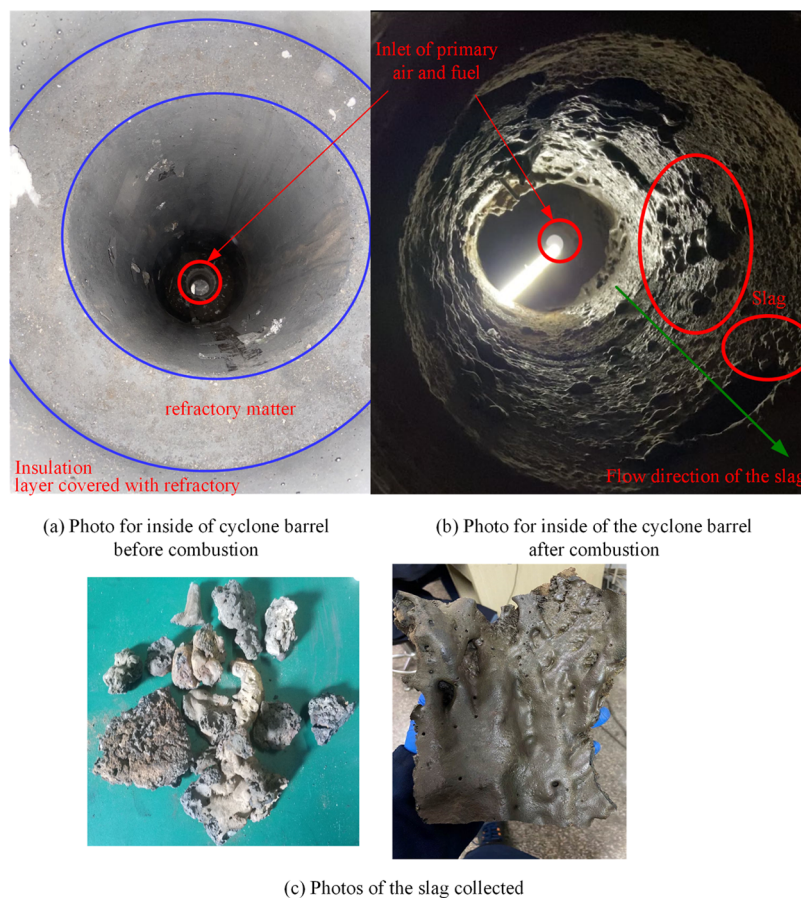


Figure 7. Pictures of the inside wall of the cyclone barrel and collected slags from the slag pool and cyclone barrel (taken by co-authors: Chunli Tang and Tao Zhu).

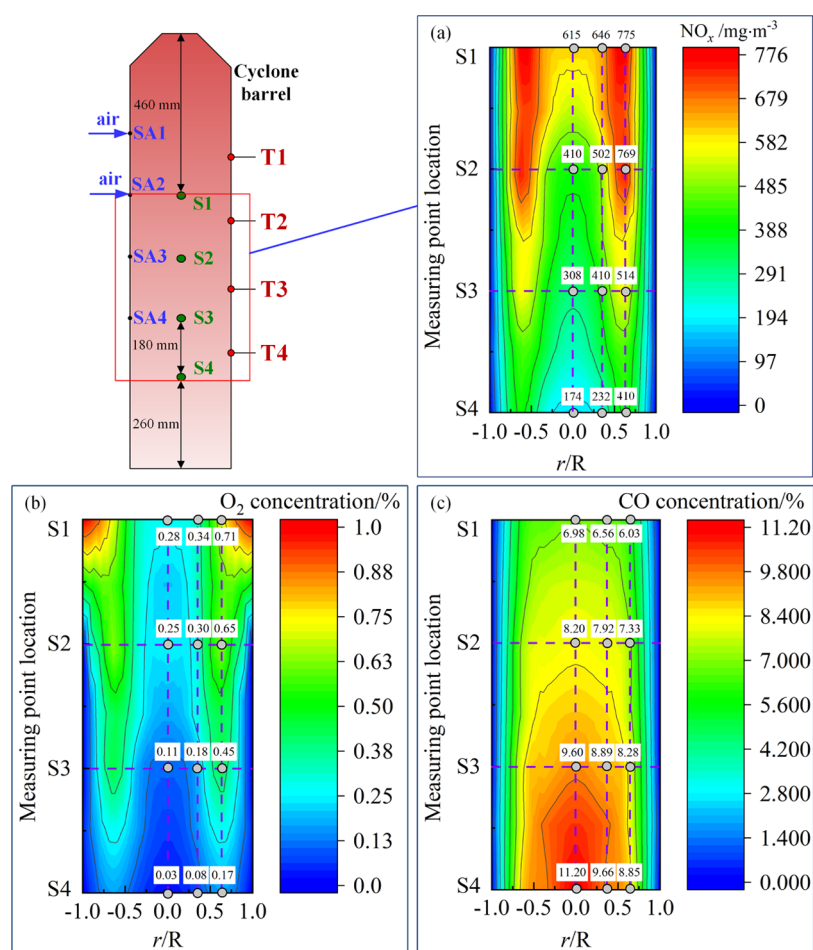


Figure 8. Species concentration distributions: (a) NO_x , (b) O_2 , and (c) CO.

melting of the slag can be clearly seen. Besides, a small part of the small particles with good following ability will follow the flue gas into the burnout chamber and burn out into ash that are captured by the cyclone ash collector. So, the mass of the slag and the ash can be weighted, respectively, and the slag capture ratio can be calculated according to the following equation

$$R = \frac{m_{\text{slag}}}{m_{\text{coal}} \times C_{\text{ash}}} \quad (3)$$

where m_{slag} and m_{coal} are, respectively, the mass of the collected slag and the coal, kg, and C_{ash} is the mass fraction of ash in coal. The slag capture ratio was 0.70 calculated by eq 3. B&W company has also indicated that the slag capture ratio can reach 0.70–0.75 under ideal operating conditions.³⁰ Therefore, a reasonable slag capture ratio can be achieved for the cyclone barrel even under air-staged conditions. Besides, the unburned carbon content of the collected fly ash is 2.8–5.4%, which indicates that the cyclone barrel has a good burnout performance under air-staged conditions.

3.3. Distributions of Species Concentrations in the Cyclone Barrel. A large volume of secondary air fed into the cyclone tangentially from the wall will result in more sufficient air in the annular near-wall region and strong swirling effects as well. The fuel in the cyclone barrel will be driven to the annular near-wall region under the action of centrifugal force. As a result, the combustion in the cyclone barrel is nonuniformly distributed, which further leads to inhomoge-

neous species concentrations. Identifying the distributions of species concentrations in the cyclone is the premise to clarify the NO_x reduction mechanism of the cyclone furnace and propose effective NO_x reduction strategies. The species concentrations are measured at different heights (S1, S2, S3, and S4 in Figure 1) of the cyclone barrel. The sampling probe takes samples at different positions away from the center axis of the cyclone barrel (0, 50, and 90 mm) to obtain a radial distribution. Figure 8 shows the concentration contours of NO_x , O_2 , and CO in the main area of the cyclone barrel under the reference condition (namely, overall-SR of 1.1, the cyclone-SR of 0.8, and the PAR of 0.3). Based on the axisymmetric characteristics of species concentration field in our previous numerical work,²⁸ the measured data²⁷ are expanded into a contour map in the longitudinal section of the cyclone barrel to better analyze the species distribution characteristics. Overall, NO_x and O_2 have a higher concentration in the annular near-wall area than in the center zone of the cyclone barrel (Figure 8a,b), while the CO in the central zone is of significantly higher concentration than that in the annular near-wall area (Figure 8c). In detail, since the intense combustion of coal particles takes place in the annular near-wall region due to more sufficient air, the coincidence of high O_2 concentration and high temperature can lead to a large amount of NO_x formation. Hence, to further reduce NO_x , the distributed air supply can be applied so as to decrease the maximal O_2 concentration in this area. Besides, since the coal particles of small size and some unburned flue gas quickly deplete the O_2 in the center region,

the main area for the NO_x reduction occurs in the middle and lower parts of the cyclone barrel with high temperature and strong reducing atmosphere. Hence, enlarging the reduction zone is conducive to reducing NO_x , which can be achieved by reducing the velocity of primary air and improving the velocity of the secondary air. Therefore, two strategies for reducing NO_x in the cyclone furnace, namely, expanding the reduction zone and reducing the oxygen concentration in the annular near-wall region, will be analyzed in Section 3.5.

3.4. NO_x Formation Characteristics. The overall-SR of the cyclone furnace determines the oxygen concentration level and directly affects the NO_x generation in the cyclone combustion process. Meanwhile, the overall-SR of the cyclone furnace is closely related to the incomplete combustion loss. So, the cases with different Overall-SRs (1.05, 1.1 and 1.2) were studied to find an appropriate overall-SR of cyclone furnace on the premise of ensuring combustion efficiency. Figure 9 shows the effects of overall-SR of the cyclone furnace

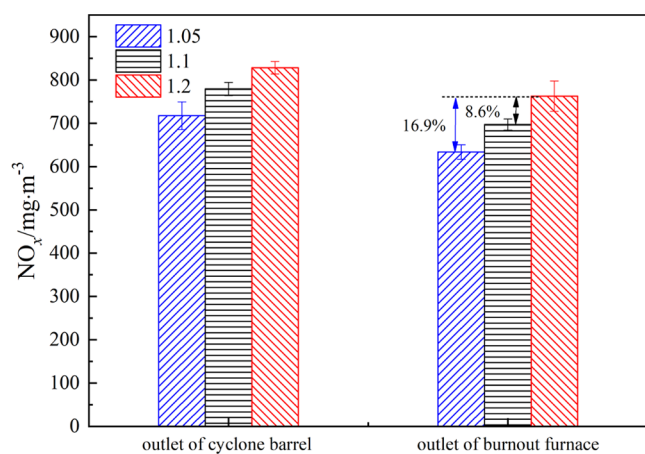


Figure 9. Effects of overall-SR of the cyclone furnace on the NO_x formation.

on the NO_x formation. If the air is fed into the cyclone barrel at one time, the sufficient oxygen inside the cyclone will lead to high levels of NO_x generation at the outlets of both the cyclone barrel and the burnout chamber. The NO_x generation at the burnout chamber outlet decreased by 8.6 and 16.9%, respectively, as overall-SR decreasing from 1.2 to 1.1 and 1.05. Although the reduction of the overall-SR can suppress the generation of NO_x to some extent, it will also decrease the combustion efficiency of the cyclone furnace. When the overall-SR is 1.05, the CO concentration at the outlet of the burnout chamber can reach $3900 \mu\text{L}\cdot\text{L}^{-1}$. In contrast, when the overall-SR is 1.1 and 1.2, the CO concentration at the outlet of the burnout chamber of the cyclone furnace is only 40 and $10 \mu\text{L}\cdot\text{L}^{-1}$, respectively. Considering both combustion efficiency and NO_x generation, the overall-SR of 1.1 is selected in the following study.

Figure 10 shows the species concentrations of NO_x , O_2 , and CO along the flue gas flow direction in a cyclone furnace under different cyclone-SR conditions. S1–S4 (arranged at 90 mm away from the central axis) are the measuring points in the annular near-wall region, and S5 and S6 are the measuring points in the transition flue and the outlet of the cyclone furnace, respectively. As shown in Figure 10a, from S1 to S5, the concentration of NO_x gradually decreases and reaches the lowest at the outlet of the cyclone barrel in the cases with SR of

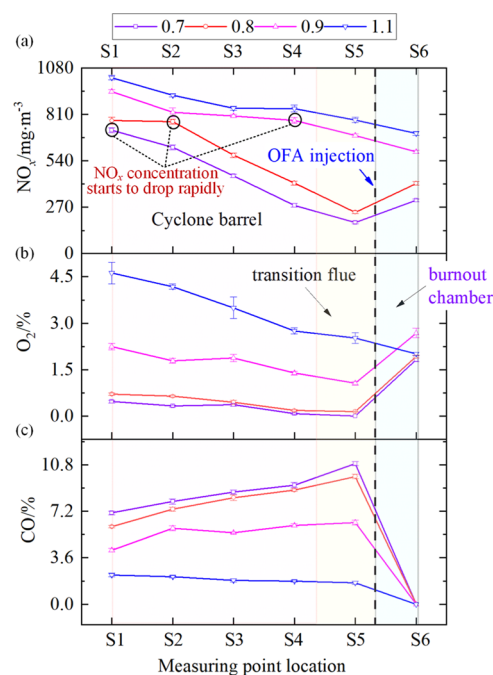


Figure 10. Species concentrations in the cyclone furnace at different cyclone-SR values.

0.7 and 0.8, but with the introduction of OFA, NO_x formation slightly increases. In the cases with cyclone-SR of 0.9 and 1.1, the NO_x concentration decreases along S1 to S6. Besides, in Figure 10b, the O_2 concentration gradually decreases from S1 to S5 when the cyclone-SR are 0.7, 0.8, and 0.9 and then increases with the injection of OFA at S6. However, when the cyclone-SR is 1.1, the O_2 concentration decreases gradually from S1 to S6. In addition, as shown in Figure 10c, CO concentration slightly decreases from S1 to S5 when the cyclone-SR is 0.7, whereas CO concentration slightly increases from S1 to S5 when the cyclone-SR is 0.8, 0.9, and 1.1. With the introduction of OFA, CO concentration decreases significantly. In this study, the combustion with the cyclone-SR of 1.1 was called nonstaged combustion, and the combustions with the cyclone-SR of 0.8 and 0.7 were called deep-air-staged combustion, and the combustion with cyclone-SR of 0.9 was called shallow-air-staged combustion.

A large amount of NO_x is formed in the upper part of the cyclone barrel. Especially for the nonstaged combustion (cyclone-SR = 1.1), the NO_x concentration in the flue gas at S₁ is as high as $1025 \text{ mg}\cdot\text{m}^{-3}$ (Figure 10a). This is mainly because the rapid pyrolysis of the pulverized coal generates a large amount of nitrogen oxide precursors (NH_3 and HCN). Meanwhile, the introduction of primary and secondary air creates a high oxygen concentration zone, and NH_3 and HCN are rapidly oxidized to NO_x . Hence, reducing the PAR can effectively decrease the initial NO_x formation. Besides, for the shallow-air-staged combustion (cyclone-SR = 0.9) and nonstaged air combustion (cyclone-SR = 1.1), with the combustion of volatile matters, the O_2 in flue gas is gradually consumed, and an oxygen-lean atmosphere would be formed in the lower zone of the cyclone barrel. The formed NO_x can not only be reduced to N_2 by the homogeneous reaction with reducing substances (NH_3 , HCN, etc.) but also be efficiently reduced by the heterogeneous reaction on the surface of char³¹ with a high concentration of CO (Figure 8c). Hence, the

concentration of NO_x shows a slight downward trend along the flue gas flow direction. In contrast, for the deep-air-staged combustion (cyclone-SR = 0.7 and 0.8), an obvious oxygen-lean atmosphere is formed as the O_2 is depleted (Figure 8b), which leads to a significant decrease in NO_x from S1 to the lowest at S5. This is due to three reasons: First, the lean of oxygen environment inhibits the oxidation of NH_3 and HCN ; second, the reduction reaction of NO_x is the dominant reaction under oxygen-lean atmospheres; and third, the strong swirling in the cyclone barrel can improve the mass transfer and promote the reduction reaction between NO_x and reducing substances. In addition, the reduction of the cyclone-SR greatly reduces the O_2 concentration in the cyclone barrel, thereby enhancing the reducing atmosphere. As the cyclone-SR decreases, the area where the NO_x reduction reaction occurs in the cyclone barrel becomes larger. In the shallow-air-staged combustion (cyclone-SR = 0.9), the reducing rate of NO_x slightly increases at S₄, indicating that NO_x reduction occurs in the lower zone of the cyclone barrel. However, in deep-air-staged combustion condition (cyclone-SR = 0.7 and 0.8), the NO_x concentration starts to drop rapidly at S₂ and S₁ when the cyclone-SR is 0.8 and 0.7, respectively, indicating that with decreasing cyclone-SR, the NO_x reduction zone in the cyclone barrel becomes larger.

As shown in Figure 11, the NO_x formation at the outlet (at S₆) of the cyclone furnace is as high as $699 \text{ mg}\cdot\text{m}^{-3}$ in

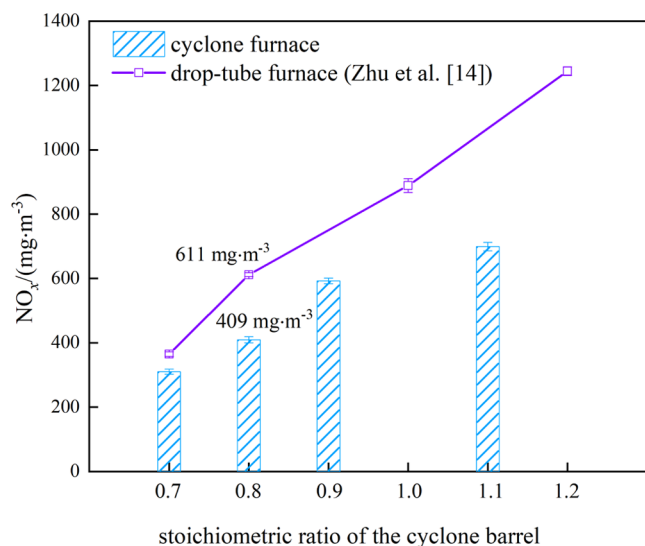


Figure 11. NO_x concentration at the outlet of the cyclone furnace.

nonstaged combustion (cyclone-SR = 1.1). The amount of NO_x formed dramatically decreases with the decrease in the cyclone-SR. When the cyclone-SR is 0.7 and 0.8, the NO_x formation drops by about 56 and 41%. When the cyclone-SR is 0.8, the NO_x formation is as low as $409 \text{ mg}\cdot\text{m}^{-3}$. In addition, the NO_x emission of the cyclone staged combustion is much lower compared with that of laminar drop-tube staged combustion in our previous study.¹⁵ In the deep-air-staged case (i.e., cyclone-SR of 0.8), the NO_x emission of cyclone furnace (with the swirl intensity of 3.74 at cyclone-SR of 0.8) is about $200 \text{ mg}\cdot\text{m}^{-3}$ lower than that of laminar drop-tube staged combustion. And in the nonstaged case, the NO_x emission of cyclone furnace (with the swirl intensity of 10.03 at cyclone-SR of 1.1) is also lower than that of the drop-tube furnace. Therefore, the strong swirling effect in the cyclone combustion

is also a conducive factor for the NO_x reduction, and the influence of swirl intensity also needs to be considered when adjusting cyclone-SR.

3.5. Low NO_x Strategies. Enlarging the reduction zone is conducive to reducing NO_x , which can be achieved by reducing PAR in addition to reducing the cyclone-SR. To clarify the effect of PAR on the NO_x formation, the concentrations of NO_x , CO, and O_2 were measured at the measuring points S1 and S5 when the PAR was 0.2, 0.3, and 0.4, respectively. The PAR was changed by adjusting the ratio of primary and secondary air when the cyclone-SR is maintained at 0.8. As shown in Figure 12, the PAR determines

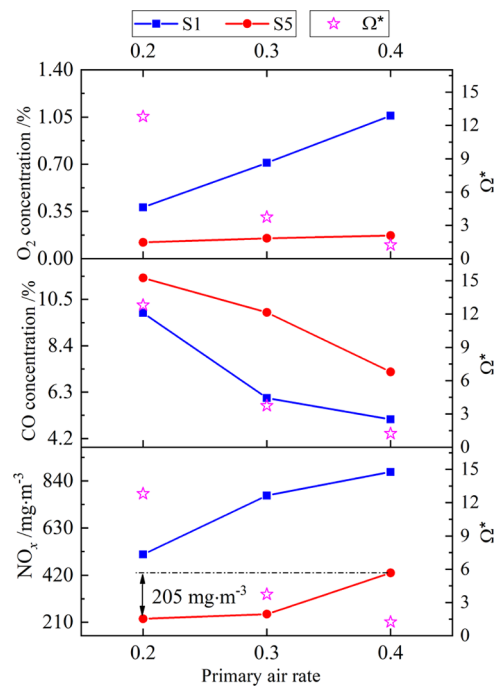


Figure 12. Effect of PAR on the species concentration at the upper and outlet of the cyclone barrel.

the O_2 concentration and significantly affects the concentrations of CO and NO_x at the top of the cyclone barrel (S1). When the PAR is reduced from 0.4 to 0.2, the swirling intensity is increased from 1.23 to 12.81. As a result, the O_2 at the S1 measuring point decreases from 1.06 to 0.38%, and the CO concentration increases from 5.07 to 9.89%, and the NO_x concentration decreases from 879.45 to $512.5 \text{ mg}\cdot\text{m}^{-3}$. When the PAR is 0.4, the NO_x at the outlet of the cyclone barrel is almost twice as much as that at the PAR of 0.2. Therefore, keeping cyclone-SR constant and reducing the PAR will greatly enhance the swirling intensity in the cyclone barrel, which not only decreases the area of high O_2 concentration but also expands the NO_x reduction zone. It should be noted that reducing the PAR will remarkably decrease the flue gas temperature, as shown in Figure 13, but the temperature near the outlet of the cyclone barrel is higher than the slag flow temperature even at the PAR of 0.2.

The O_2 concentration in the annular near-wall region can be reduced by adjusting the centralized air supply (SA1 + SA2) to decentralized air supply (SA1 + SA3). To identify the species distribution characteristics influenced by the secondary air arrangement in the cyclone barrel, the concentrations of O_2 , CO, and NO_x were measured at measuring points S1, S2, S3,

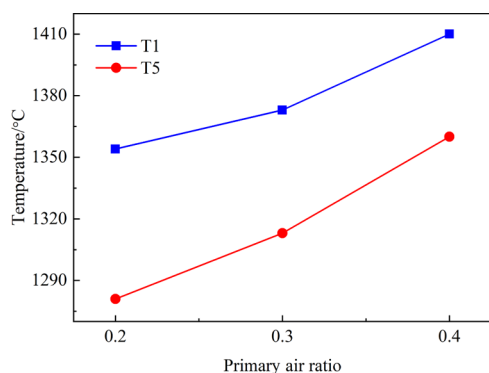


Figure 13. Effect of PAR on the temperature at the upper part and outlet of the cyclone barrel.

S4, and S5 in the cases of centralized secondary air supply and decentralized secondary air supply. As shown in Figure 14,

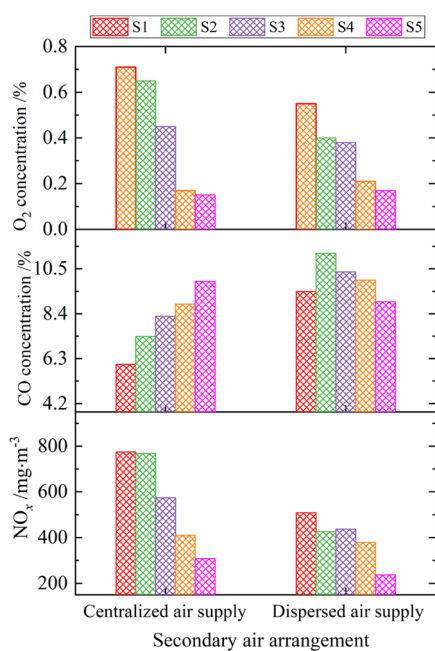


Figure 14. Species concentrations in the near-wall region affected by secondary air arrangement.

compared with the case with centralized air supply, O₂ concentration in the annular near-wall region (S1–S4) is significantly reduced in the case of decentralized secondary air supply, resulting a decreased NO_x formation. This is because the decentralized air supply can effectively avoid the excess of O₂, reducing the NO_x formation. At the cyclone outlet (S5), although O₂ concentrations remain almost constant between decentralized air supply and centralized air supply, the NO_x concentration of decentralized air supply is 236 mg·m⁻³, which is about 23% lower. Therefore, decentralized secondary air supply is an effective approach to reduce the O₂ concentration in the annular near-wall region and further to reduce NO_x formation. Figure 15 shows the effect of secondary air arrangement on the temperature at the upper part and outlet of the cyclone barrel. It is found that decentralized secondary air supply would slightly reduce the temperature in the cyclone. However, the temperature at the outlet of the cyclone

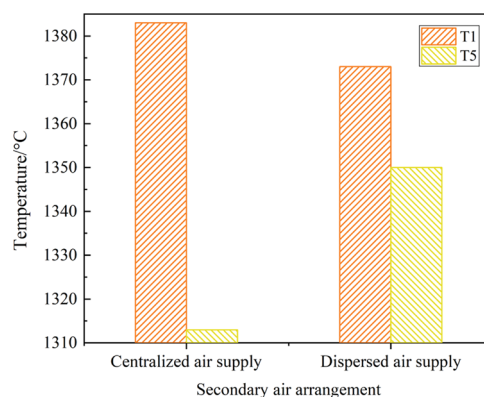


Figure 15. Effect of secondary air arrangement on the temperature at the upper part and outlet of the cyclone barrel.

barrel can be increased by the decentralized secondary air supply, which is more conducive to the slag tapping.

4. CONCLUSIONS

In this study, a 100 kW cyclone furnace experimental system was built to study the combustion characteristics and their effects on NO_x formation in the cyclone barrel. The main conclusions can be drawn as follows:

- (1) In the annular near-wall region of the cyclone barrel, the coincidence of high O₂ concentration and high temperature can lead to a large amount of NO_x formation. Besides, NO_x reduction area with high temperatures and high CO concentrations would significantly promote the reduction of NO_x in the central and lower parts of the cyclone barrel. To expand the reduction zone and to reduce O₂ concentration in the annular near-wall region are two effective strategies for reducing NO_x in the cyclone furnace.
- (2) A reasonable slag capture ratio of 0.70 can be achieved for the cyclone barrel even under air-staged conditions. The unburned carbon content of the collected fly ash is 2.8–5.4%. The cyclone furnace shows good slag capture and burnout performance even in air-staged cases.
- (3) The overall-SR cannot be too small to impact the burnout performance of cyclone furnace, so it has limited effects on the reduction of NO_x emission. In contrast, NO_x formation can be significantly dropped by 56% when the cyclone-SR decreases from 1.1 to 0.7.
- (4) Keeping cyclone-SR constant and reducing the primary air rate will greatly enhance the swirling intensity in the cyclone barrel, which not only decreases the area of high O₂ concentration but also expands the NO_x reduction zone. The oxygen concentration can be reduced in the annular near-wall region by decentralizing the secondary air supply, thereby inhibiting the NO_x formation by 23%.
- (5) The NO_x emission of cyclone staged combustion is lower than that of laminar drop-tube staged combustion in either air-staged or nonstaged cases, which can be attributed to the swirling effect.
- (6) The detailed data including temperature profiles, species concentration distributions, and slag tapping behavior of the cyclone furnace can be used as the reference for the verification of the future numerical study.

AUTHOR INFORMATION

Corresponding Author

Chunli Tang – School of Human Settlements and Civil Engineering, Xi'an Jiaotong University, Xi'an 710049, China; orcid.org/0000-0003-3007-541X; Email: tangchunli219@163.com

Authors

Limin Wang – State Key Laboratory of Multiphase Flow in Power Engineering, School of Energy and Power Engineering, Xi'an Jiaotong University, Xi'an 710049, China

Tao Zhu – State Key Laboratory of Multiphase Flow in Power Engineering, School of Energy and Power Engineering, Xi'an Jiaotong University, Xi'an 710049, China

Fan Fang – Xi'an Thermal Power Research Institute CO., LTD., Xi'an, Shaanxi 710054, China

Xing Ning – State Key Laboratory of Multiphase Flow in Power Engineering, School of Energy and Power Engineering, Xi'an Jiaotong University, Xi'an 710049, China

Defu Che – State Key Laboratory of Multiphase Flow in Power Engineering, School of Energy and Power Engineering, Xi'an Jiaotong University, Xi'an 710049, China; orcid.org/0000-0003-1881-4136

Complete contact information is available at: <https://pubs.acs.org/10.1021/acsomega.2c02689>

Notes

The authors declare no competing financial interest.

ACKNOWLEDGMENTS

This work was financially supported by the Shaanxi Provincial Natural Science Basic Research Program under grant no. 2021JQ-045, China Postdoctoral Science Foundation under grant no. 2018M643643, and National Key Research and Development Program of China under grant no. 2018YFB0604103.

REFERENCES

- (1) Wu, X.; Zhang, X.; Yan, K.; Chen, N.; Zhang, J.; Xu, X.; Dai, B.; Zhang, J.; Zhang, L. Ash deposition and slagging behavior of Chinese Xinjiang high-alkali coal in 3 MWth pilot-scale combustion test. *Fuel* **2016**, *181*, 1191–1202.
- (2) Fan, H. L.; Feng-Hai, L. L.; Mei-Ling, X. U.; Huang, J. J. Research progress of adjustment of melting temperature for coal ash with a low ash melting point. *Appl. Chem. Ind.* **2016**, *45*, 1372–1375.
- (3) Wang, W.; Sun, Y.; Huang, Z.; Liao, Y.; Fang, F. Numerical Simulation of NO_x Emission Characteristics of a Cyclone Boiler with Slag-Tap Furnace. *ACS Omega* **2020**, *5*, 29978–29987.
- (4) Zhou, Z.; Bo, Y.; Zhang, Y.; Huang, Z.; Chen, L.; Ge, L.; Zhou, J.; Cen, K. Interactions of high-chromia refractory materials with infiltrating coal slag in the oxidizing atmosphere of a cyclone furnace. *Ceram. Int.* **2014**, *40*, 3829–3839.
- (5) Wu, S.; Deng, L.; Wang, C. A.; Tang, C.; Bu, Y.; Che, D. A Study on the Adaptability of Cyclone Barrel to Slag Film in a Cyclone-fired Boiler. *Appl. Therm. Eng.* **2017**, *121*, 368–379.
- (6) Tang, C.; Deng, L.; Wu, S.; Bu, Y.; Che, D. Numerical simulation on the slag flow and heat transfer characteristics of the cyclone barrel for a cyclone-fired boiler. *Numer. Heat Transfer, Part A* **2017**, *71*, 1052–1065.
- (7) Spliethoff, H.; Greul, U.; Rüdiger, H.; Hein, K. R. G. Basic effects on NO_x emissions in air staging and reburning at a bench-scale test facility. *Fuel* **1996**, *75*, 560–564.
- (8) Fei, J.; Sun, R.; Yu, L.; Liao, J.; Sun, S.; Kelebopile, L.; Qin, Y. NO Emission Characteristics of Low-Rank Pulverized Bituminous

Coal in the Primary Combustion Zone of a Drop-Tube Furnace. *Energy Fuels* **2010**, *24*, 3471–3478.

(9) Sirisomboon, K.; Charemporn, P. Effects of air staging on emission characteristics in a conical fluidized-bed combustor firing with sunflower shells. *J. Energy Inst.* **2017**, *90*, 316–323.

(10) Fei, J.; Sun, R.; Yu, L.; Liao, J.; Sun, S.; Kelebopile, L.; Qin, Y. NO Emission Characteristics of Low-Rank Pulverized Bituminous Coal in the Primary Combustion Zone of a Drop-Tube Furnace. *Energy Fuels* **2010**, *24*, 3471–3478.

(11) Taniguchi, M.; Kamikawa, Y.; Okazaki, T.; Yamamoto, K.; Orita, H. A role of hydrocarbon reaction for NO_x formation and reduction in fuel-rich pulverized coal combustion. *Combust. Flame* **2010**, *157*, 1456–1466.

(12) Zhang, W.; Li, Y.; Ma, X.; Qian, Y.; Wang, Z. Simultaneous NO/CO₂ removal performance of biochar/limestone in calcium looping process. *Fuel* **2020**, *262*, No. 116428.

(13) Zhao, Y.; Feng, D.; Li, B.; Wang, P.; Tan, H.; Sun, S. Effects of flue gases (CO/CO₂/SO₂/H₂O/O₂) on NO-Char interaction at high temperatures. *Energy* **2019**, *174*, 519–525.

(14) Zha, Q.; Bu, Y.; Wang, C. A.; Che, D. Evaluation of anthracite combustion and NO_x emissions under oxygen-staging, high-temperature conditions. *Applied Thermal Engineering* **2016**, *109*, 751–760.

(15) Zhu, T.; Hu, Y.; Tang, C.; Wang, L.; Liu, X.; Deng, L.; Che, D. Experimental study on NO_x formation and burnout characteristics of pulverized coal in oxygen enriched and deep-staging combustion. *Fuel* **2020**, *272*, No. 117639.

(16) Taniguchi, M.; Kamikawa, Y.; Tatsumi, T.; Yamamoto, K. Staged combustion properties for pulverized coals at high temperature. *Combust. Flame* **2011**, *158*, 2261–2271.

(17) Bai, W.; Li, H.; Deng, L.; Liu, H.; Che, D. Air-Staged Combustion Characteristics of Pulverized Coal under High Temperature and Strong Reducing Atmosphere Conditions. *Energy Fuels* **2014**, *28*, 1820–1828.

(18) Jones, J. M.; Pourkashanian, M.; Waldron, D. J.; Williams, A. Prediction of NO_x and unburned carbon in ash in highly staged pulverised coal furnace using overfire air. *J. Energy Inst.* **2010**, *83*, 144–150.

(19) Zhu, S.; Lyu, Q.; Zhu, J. Experimental investigation of NO_x emissions during pulverized char combustion in oxygen-enriched air preheated with a circulating fluidized bed. *Journal of the Energy Institute* **2019**, *92*, 1388–1398.

(20) Song, G.; Yang, X.; Yang, Z.; Xiao, Y. Experimental study on ultra-low initial NO_x emission characteristics of Shenmu coal and char in a high temperature CFB with post-combustion. *Journal of the Energy Institute* **2021**, *94*, 310–318.

(21) Krasinsky, D. V.; Salomatov, V. V.; Anufriev, I. S.; Sharypov, O. V.; Shadrin, E. Y.; Anikin, Y. A. Modeling of pulverized coal combustion processes in a vortex furnace of improved design. Part 1: Flow aerodynamics in a vortex furnace. *Thermal Engineering* **2015**, *62*, 117–122.

(22) Krasinsky, D. V.; Salomatov, V. V.; Anufriev, I. S.; Sharypov, O. V.; Shadrin, E. Y.; Anikin, Y. A. Modeling of pulverized coal combustion processes in a vortex furnace of improved design. Part 2: Combustion of brown coal from the Kansk-Achinsk Basin in a vortex furnace. *Thermal Engineering* **2015**, *62*, 208–214.

(23) Lani, B. W.; Feeley, T. J.; Miller, C. E.; Carney, B. A.; Murphy, J. T. DOE/NETL's NO_x emissions control R&D program - bringing advanced technology to the marketplace, 2008.

(24) Sarv, H.; Sayre, A. N.; Maringo, G. J. In *Selective Use of Oxygen and In-furnace Combustion Techniques for NO_x Reduction in Coal Burning Cyclone Boilers*, 33rd International Technical Conference on Coal Utilization & Fuel Systems, Clearwater, Florida, 2008; p 1809.

(25) Farzan, H.; Maringo, G. J.; Johnson, D. W.; Wong, D. K.; Beard, C. T.; Brewster, S. E. *B&W Advances on Cyclone NO_x Control via Fuel and Air Staging Technologies*, EPRI-DOE-EPA Combined Utility Air Pollutant Control, Atlanta, Georgia, 1999; p 1683.

(26) Sarv, H.; Chen, Z.; Sayre, A.; Maringo, G.; Levesque, S. *Oxygen-Enriched Combustion of a Powder River Basin Black Thunder Coal for*

NOx Reduction in a Cyclone Furnace, The 34th International Technical Conference on Clean Coal and Fuel Systems, Florida, USA, 2009.

(27) Zhu, T.; Tang, C.; Ning, X.; Wang, L.; Deng, L.; Che, D. Experimental study on NO_x emission characteristics of Zhundong coal in cyclone furnace. *Fuel* **2022**, *311*, No. 122536.

(28) Tang, C.; Zhu, T.; Hu, Y.; Wang, L.; Che, D.; Liu, Y. Numerical Investigation of the Effects of Swirl-Vane Angle and Particle Size on Combustion and Flow Characteristics in a Vertical Cyclone Barrel. *J. Energy Eng.* **2020**, *146*, No. 04020029.

(29) Tang, C.; Zhu, T.; Wang, L.; Deng, L.; Che, D.; Liu, Y. Effects of ash parameters and fluxing agent on slag layer behavior in cyclone barrel. *Fuel* **2019**, *253*, 1140–1148.

(30) Kitto, J. B.; Stultz, S. C. *Steam - Its Generation and Use*; Babcock & Wilcox Company, 2005.

(31) Wang, C. A.; Du, Y.; Che, D. Investigation on the NO Reduction with Coal Char and High Concentration CO during Oxy-fuel Combustion. *Energy Fuels* **2012**, *26*, 7367–7377.